Synthesis, Molecular Structures, and Fluxional Behavior of dppm-Bridged Complexes of Platinum(II) with Linear Gold(I), Trigonal Silver(I), or Tetrahedral Mercury(II) Centers

Chongfu Xu, Gordon K. Anderson,* Lee Brammer, Janet Braddock-Wilking, and Nigam P. Rath

Department of Chemistry, University of Missouri−St. Louis, 8001 Natural Bridge Road, St. Louis, Missouri 63121

Received May 13, 1996[⊗]

The complexes [PtR(dppm-*P*,*P*)(dppm-*P*)]PF_6 (R = Me, Et, Ph) react with [AuCl(SMe_2)] to generate the dppm-bridged platinum−gold complexes *trans*-[PtClR(μ-dppm)$_2$Au]PF_6 (**1**). Addition of [PtR(dppm-*P*,*P*)(dppm-*P*)]Cl to a solution of silver(I) acetate, followed by acetyl chloride, yields the neutral platinum-silver species *trans*-[PtClR(μ-dppm)$_2$AgCl] (**2**). Similarly, addition of [PtR(dppm-*P*,*P*)(dppm-*P*)]Cl to a solution of mercury(II) acetate, followed by acetyl chloride, yields the neutral platinum-mercury species *trans*-[PtClR(μ-dppm)$_2$$HgCl_2$] (**3**). Each of the complexes has been characterized by ^{1}H and ^{31}P{^{1}H} NMR spectroscopy and by elemental analysis. The crystal structure of **1** as its methyl derivative **1a** ($CHCl_3$ solvate) has been determined by X-ray diffraction. The compound exhibits approximate square-planar geometry at platinum and linear geometry at gold. The platinum−gold internuclear distance is 3.008(1) Å. The methyl complex **2a** crystallizes as its $CHCl_3$ solvate. The geometry at platinum is distorted square planar, and the Pt···Ag distance is 3.049(1) Å. The geometry at silver is approximately trigonal planar. The pyramidal distortion taken together with a long Ag−Cl bond (2.610(4) Å) is discussed in the context of C−H···Cl hydrogen bonding and a possible incipient Pt···Ag interaction. The structure of **3a** was also determined by X-ray diffraction. The geometry at platinum is distorted square planar, and the Pt···Hg distance is 3.302(1) Å. The geometry at mercury can be described as pyramidally distorted tetrahedral. However, taken together with an unusually long axial Hg−Cl distance (2.715(4) Å), this distortion may be viewed in terms of an incipient S_N2 reaction at the Hg center that invokes a weak Pt···Hg interaction. The complexes have static structures at ambient temperature, as evidenced by the nonequivalence of the methylene hydrogens of the dppm ligands, but they exhibit fluxional behavior at higher temperatures. Free energies of activation in the range 13−19 kcal/mol have been determined, being higher for the Pt-Au species, and a mechanism involving reversible dissociation of chloride is proposed to account for the observed behavior.

Introduction

The use of bis(diphenylphosphino)methane (dppm) or related ligands in the construction of bimetallic and trimetallic complexes has developed tremendously over the last 20 years, and a number of reviews of this area have appeared.[1−6] In particular, dppm-bridged complexes of platinum or palladium have received considerable attention, including A-frame species that contain a bridging group such as a halide, hydride, CH_2, CO, S, SO_2, or another metal. Several methods have been utilized in the preparation of such species, but in most, if not all, cases the synthetic methods have been limited to the preparation of symmetrical complexes. We have reported recently the use of organoplatinum species of the type [PtR(dppm-*P*,*P*)(dppm-*P*)]PF_6 in the synthesis of unsymmetrical chloride- and hydride-bridged diplatinum or platinum-palladium complexes.[7,8] In this paper we describe an extension of the use of these organoplatinum cations to the preparation of heterobimetallic complexes of platinum with gold, silver, and mercury.

A number of complexes of platinum and one of these metals have been reported previously, notably by Shaw and co-workers, in most cases prepared from platinum complexes containing two monodentate dppm ligands, although in certain instances the bis(chelate) complex [Pt(dppm-*P*,*P*)$_2$]Cl_2 was employed.[9−13]

[⊗] Abstract published in *Advance ACS Abstracts,* August 15, 1996.

(1) Puddephatt, R. J. *Chem. Soc. Rev.* **1983**, *12*, 99.
(2) Balch, A. L. In *Homogeneous Catalysis with Metal Phosphine Complexes*; Pignolet, L. H., Ed., Plenum: New York, 1983; pp 167−213.
(3) Balch, A. L. *Comments Inorg. Chem.* **1984**, *3*, 51.
(4) Chaudret, B.; Delavaux, B.; Poilblanc, R. *Coord. Chem. Rev.* **1988**, *86*, 191.
(5) Puddephatt, R. J.; Manojlovic-Muir, L.; Muir, K. W. *Polyhedron* **1990**, *9*, 2767.
(6) Anderson, G. K. *Adv. Organomet. Chem.* **1993**, *35*, 1.
(7) Fallis, K. A.; Xu, C.; Anderson, G. K. *Organometallics* **1993**, *12*, 2243.
(8) Xu, C.; Anderson, G. K. *Organometallics* **1994**, *13*, 3981.
(9) Hassan, F. S. M.; Markham, D. P.; Pringle, P. G.; Shaw, B. L. *J. Chem. Soc., Dalton Trans.* **1985**, 279.

S0276-7333(96)00355-X CCC: $12.00

Results and Discussion

Synthesis and Characterization. When [AuCl(SMe$_2$)] was treated with 1 mol equiv of [PtMe(dppm-*P,P*)(dppm-*P*)]PF$_6$ in dichloromethane solution, followed by addition of excess NH_4PF_6, the heterobimetallic complex *trans*-[PtClMe(μ-dppm)$_2$Au]PF$_6$ (**1a**) was formed. It was isolated in excellent yield as a pale yellow solid following purification. The ethyl- and phenylplatinum analogues (**1b,c**) were prepared similarly (eq 1). Each

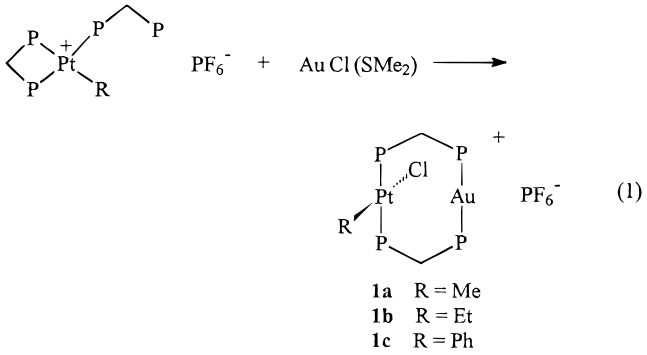

(1)

1a R = Me
1b R = Et
1c R = Ph

compound was characterized by elemental analysis and by NMR spectroscopy, and **1a** has been the subject of an X-ray diffraction study. The $^{31}P\{^1H\}$ NMR spectrum of **1a** consists of two apparent triplets, the separation of the outer lines of which is given by $|^2J(P_a,P_b) + {}^4J(P_a,P_d)|$[10,11] Each resonance is flanked by ^{195}Pt satellites, one with a coupling constant of 3049 Hz, due to the P atom attached to platinum, and one with a long-range coupling of 126 Hz, due to the P atom bonded to gold. The $^{31}P\{^1H\}$ NMR spectra of **1b**,**c** are qualitatively similar, although the ethyl complex exhibits a larger ^1J(Pt,P) value, as we have observed previously in diplatinum and platinum-palladium dppm-bridged complexes.[7] The ^1J(Pt,P) values are typical of *trans*-PtClRP$_2$ moieties. The ^3J(Pt,P) values of 126−142 Hz are slightly smaller than that found in [Pt(CH$_2$CH$_2$CH$_2$CH$_2$)(μ-dppm)$_2$Au]$^+$ (where the dppm ligands adopt a *cis* configuration at platinum),[11] slightly larger than that in *trans*-[Pt(C≡CPh)(CNBu^t)(μ-dppm)$_2$AuCl]$^+$,[10] and considerably larger than those in *trans*-[Pt(CN)$_2$(μ-dppm)$_2$Au]$^+$ and *trans*-[PtCl(CNBu^t)(μ-dppm)$_2$AuCl]$^+$.[9,10] Thus, there is no clear dependence of ^3J(Pt,P) on the geometry at platinum or on whether the gold center is two- or three-coordinate. The ^1H NMR spectrum of **1a** consists of a triplet at 0.47 ppm, with a 78 Hz coupling to ^{195}Pt, due to the methyl group, two broad signals due to the dppm CH$_2$ hydrogens, and resonances due to the phenyl hydrogens. The ^1H NMR spectra of **1b**,**c** also exhibit two broad resonances for the methylene groups of the dppm ligands.

The platinum-silver complexes *trans*-[PtClR(μ-dppm)$_2$AgCl] (**2a**−**c**) were prepared by addition of [PtR(dppm-*P,P*)(dppm-*P*)]Cl (R = Me, Et, Ph) to a suspension of silver(I) acetate in dichloromethane. In each case, a clear, yellow solution formed initially, whose ^{31}P NMR spectrum contained two sets of similar signals (δ(P) 23.5 dd, ^1J(Pt,P) = 3030 Hz, δ(P) −8.6 d of multiplets, ^1J(Ag,P) = *ca.* 460 Hz; δ(P) 25.7 dd, ^1J(Pt,P) = 3075 Hz, δ(P) −2.4 d of multiplets, ^1J(Ag,P) = *ca.* 445 Hz), indicating the presence of two related species. These have been tentatively identified as *trans*-[PtClR(μ-dppm)$_2$Ag(OAc)] and *trans*-[Pt(OAc)R(μ-dppm)$_2$AgCl]. Further addition of a CH$_2$Cl$_2$ solution of acetyl chloride produced a colorless solution from which the product was isolated in high yield as a white powder (eq 2). A

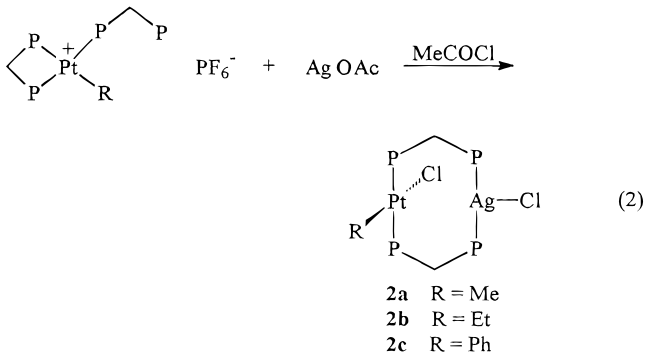

(2)

2a R = Me
2b R = Et
2c R = Ph

large excess of acetyl chloride resulted in destruction of the bimetallic complex and formation of [PtCl$_2$(dppm)]. Use of [PtMe(dppm-*P,P*)(dppm-*P*)]PF$_6$ instead of its chloride salt did not produce **2a**, indicating that the chloride ion is incorporated into the final product. Treatment of a solution of **2a** with NH_4PF_6 caused decomposition of the complex, which suggests that in solution the complex is neutral rather than consists of an organometallic cation and a free chloride counterion.

The compounds **2a**−**c** were characterized by microanalysis, ^1H and $^{31}P\{^1H\}$ NMR spectroscopy, and, in the case of **2a**, X-ray crystallography. The ^1H NMR spectra of **2a**−**c** are unremarkable, with two broad CH$_2$ resonances, separated in each case by 1.1 ppm, due to the dppm ligands. The $^{31}P\{^1H\}$ NMR spectra each consist of a doublet of doublets for the P atoms coordinated to platinum (see Experimental Section), and a complex multiplet for the P atoms attached to silver. The ^1J(Pt,P) couplings are around 3030 Hz for **2a** and **2c** and are over 200 Hz larger for **2b**, an observation analogous to that made for the Pt−Au species. The ^1J(Ag,P) couplings can also be determined, couplings to ^{109}Ag and ^{107}Ag being 460 and 400 Hz, respectively, in each case. The ^1J(Ag,P) coupling constants are similar to those observed for *trans*-[PtX(C≡CPh)(μ-dppm)$_2$AgCl] (X = Cl, C≡CPh)[12] but smaller than those in *trans*-[Pt(C≡CPh)$_2$(μ-dppm)$_2$Ag]PF$_6$[12] and [Pt(CH$_2$CH$_2$CH$_2$CH$_2$)(μ-dppm)$_2$Ag]PF$_6$,[11] again consistent with a three-coordinate silver center. The ^3J(Pt,P) coupling constants could not be determined in the present Pt−Ag complexes.

The platinum-mercury complexes *trans*-[PtClR(μ-dppm)$_2$HgCl$_2$] (**3a**−**c**; R = Me, Et, Ph) were prepared similarly by treating a suspension of mercury(II) acetate with [PtR(dppm-*P,P*)(dppm-*P*)]Cl, followed by addition of acetyl chloride. In this case several species were detected by NMR spectroscopy initially, but following addition of CH$_3$COCl the desired products were obtained in good yield (eq 3). Compounds **3a**−**c** were character-

(10) Langrick, C. R.; Pringle, P. G.; Shaw, B. L. *J. Chem. Soc., Dalton Trans.* **1984**, 1233.
(11) Pringle, P. G.; Shaw, B. L. *J. Chem. Soc., Dalton Trans.* **1984**, 849.
(12) Cooper, G. R.; Hutton, A. T.; Langrick, C. R.; McEwan, D. M.; Pringle, P. G.; Shaw, B. L. *J. Chem. Soc., Dalton Trans.* **1984**, 855.
(13) Langrick, C. R.; McEwan, D. M.; Pringle, P. G.; Shaw, B. L. *J. Chem. Soc., Dalton Trans.* **1983**, 2487.

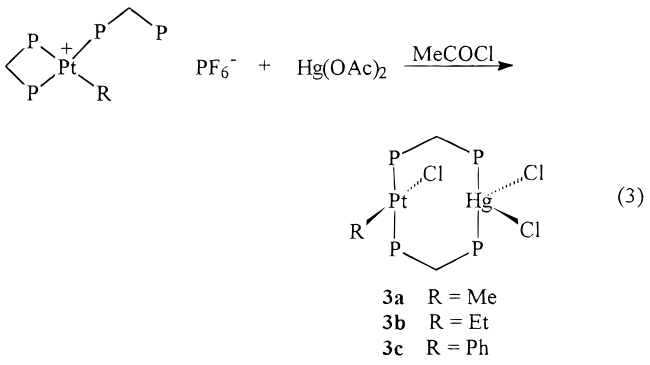

(3)

ized by elemental analysis and NMR spectroscopy. The structure of **3a** was determined by X-ray crystallography. The ^{1}H NMR spectra of **3a**,**b** show the expected signals for the alkyl groups, and all three complexes exhibit two broad resonances, separated by about 1 ppm, for the ligand CH_2 groups. The $^{31}P\{^1H\}$ NMR spectra of **3a**−**c** each consist of two apparent triplets. The high-frequency resonance exhibits a short-range coupling to ^{195}Pt of over 3000 Hz, indicating that it is due to the P atoms bonded directly to platinum, and a long-range coupling to ^{199}Hg of around 50 Hz. The low-frequency signal due to the P atoms coordinated to mercury shows a ^1J(Hg,P) value of 5600−5700 Hz and a ^3J(Pt,P) coupling of around 200 Hz. The chemical shifts and coupling constants are consistent with those found for P atoms coordinated to a $HgCl_2$ moiety in related dppm-bridged platinum-mercury compounds.[9,13]

X-ray Structure Determinations. The crystal structures of [PtClMe(μ-dppm)$_2$Au]PF_6·$CHCl_3$ (**1a**·$CHCl_3$), [PtClMe(μ-dppm)$_2$AgCl]·$CHCl_3$ (**2a**·$CHCl_3$), and [PtClMe(μ-dppm)$_2HgCl_2$] (**3a**) have been determined by X-ray diffraction. Pertinent interatomic distances and angles are presented in Table 1. The molecular structures of [PtClMe(μ-dppm)$_2$Au]$^+$, [PtClMe(μ-dppm)$_2$AgCl], and [PtClMe(μ-dppm)$_2HgCl_2$] are shown in Figure 1.

In each structure the square-planar platinum center is linked via two dppm bridges to a second metal center, which has an approximately linear (Au), trigonal (Ag), or tetrahedral (Hg) coordination environment. The diphosphine ligands are disposed in a *trans* configuration at Pt but show sufficient flexibility to accommodate the different coordination geometries presented by the second metal center (Table 1). Each of the PtClMe(P−C−P)$_2MCl_n$ cores shows approximate mirror symmetry through the mean plane of the two metals, the Cl and Me substituents of Pt, and the Cl ligands of M. Thus, the orientation of the methylene groups of the dppm ligands gives rise to a boat conformation of the Pt(P−C−P)$_2$M ring in each case.

This boat conformation may result from any, or in part from all, of a number of factors. The positions of the phenyl groups must in part be dictated by packing forces and are inevitably related to the Pt(P−C−P)$_2$M ring conformation, such that the former may exert constraints on the latter. Further, it is interesting to note that in each structure the square plane of the ligands at Pt is tilted such that Cl(1) is moved toward the other metal center; *i.e.*, the angle M···Pt−Cl(1) is less than 90°. While it is tempting to then invoke Pt−Cl(1)···M bridging interactions, the long Cl(1)···M separations (3.113 Å for **1a** and >3.5 Å for **2a**, **3a**) suggest

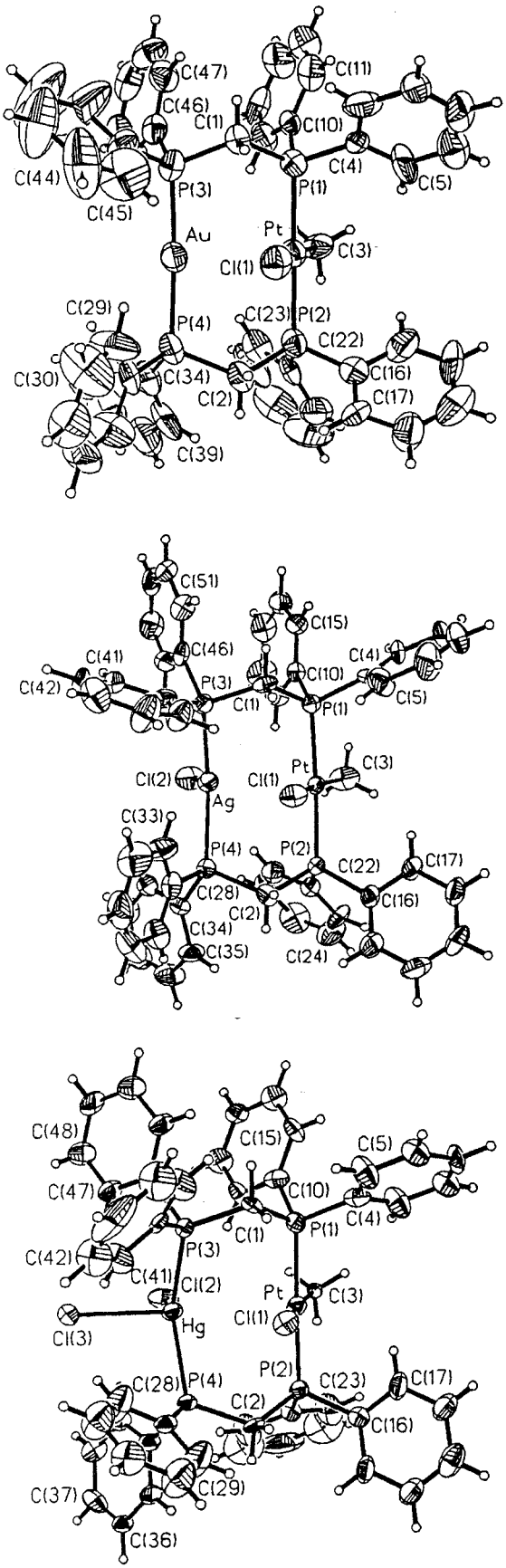

Figure 1. (Top to bottom) Molecular structures of [PtClMe(μ-dppm)$_2$Au]$^+$ (**1,** cation), [PtClMe(μ-dppm)$_2$AgCl] (**2**), and [PtClMe(μ-dppm)$_2HgCl_2$] (**3**) shown with 50% probability ellipsoids for non-hydrogen atoms.

that this is not the case. The tilting may simply result from a minimization of repulsive interactions between

Table 1. Selected Interatomic Distances (Å) and Angles (deg) for 1−3

	1	2	3
Pt···M	3.008(1)	3.049(1)	3.302(1)
Pt−P(1)	2.294(5)	2.302(3)	2.269(4)
Pt−P(2)	2.297(5)	2.294(3)	2.286(4)
Pt−Cl(1)	2.425(5)	2.420(3)	2.416(4)
Pt−C(3)	2.10(2)	2.045(10)	2.190(12)
M−P(3)	2.317(5)	2.488(3)	2.506(4)
M−P(4)	2.304(6)	2.513(3)	2.487(4)
M···Cl(1)	3.113(5)	3.570(3)	3.524(5)
M−Cl(2)		2.610(4)	2.531(5)
M−Cl(3)			2.715(4)
P(1)−C(1)	1.85(2)	1.840(10)	1.835(14)
P(3)−C(1)	1.81(2)	1.849(11)	1.814(14)
P(2)−C(2)	1.83(2)	1.834(10)	1.84(2)
P(4)−C(2)	1.86(2)	1.849(10)	1.84(2)
P−C(Ph)	1.78(2)−1.83(2)	1.797(10)−1.836(11)	1.811(8)−1.839(9)
P(1)−Pt−P(2)	175.2(2)	176.9(1)	176.2(2)
Cl(1)−Pt−C(3)	172.1(5)	170.4(4)	173.2(4)
Cl(1)−Pt−P(1)	87.8(2)	90.8(1)	89.0(2)
Cl(1)−Pt−P(2)	87.7(2)	89.0(1)	87.4(2)
C(3)−Pt−P(1)	92.6(5)	91.0(4)	89.9(4)
C(3)−Pt−P(2)	91.8(5)	89.8(4)	93.4(4)
P(3)−M−P(4)	170.8(2)	134.3(1)	135.9(1)
Cl(2)−M−P(3)		115.1(1)	111.1(1)
Cl(2)−M−P(4)		108.4(1)	111.1(1)
Cl(2)−M−Cl(3)			90.9(2)
Cl(3)−M−P(3)			95.5(1)
Cl(3)−M−P(4)			96.1(1)
M···Pt−Cl(1)	68.9(1)	80.6(1)	74.3(1)
Pt−Cl(1)···M	64.4(1)	57.4(1)	64.4(1)

the methyl ligand and the two phenyl groups of the dppm ligands (Figure 1). However, in each structure the Cl ligand on platinum is well-positioned to maximize any stabilization that may be gained from weak *intra*molecular hydrogen bonding (Table 2) involving the methylene hydrogens of the dppm ligands, and such interactions may contribute to stabilization of the boat conformer. Details of all *intra*- and other *inter*molecular C−H···X (X = F, Cl) hydrogen bonds are given in Table 2 and are depicted in Figure 2.

The widespread presence of "soft" C−H···X hydrogen bonds (particularly X = O[14] and also X = F,[15] Cl[16]) in the crystal structures of organometallic complexes has begun to receive attention in recent years, especially with reference to efforts in supramolecular design[17] and crystal engineering.[18] The presence of such interactions in the crystal structures presented here also warrants further discussion. The compound **1a**·$CHCl_3$ exhibits intermolecular C−H···F hydrogen bonding linking both the chloroform solvate and one of the methylene groups of the cation to the PF_6^- anion. A longer (weaker) C−H···Cl interaction (not shown in Figure 2) links molecules of **3a** via a methylene C−H group and the axial chloride, Cl(2), associated with the Hg center. The participation of the methylene C−H groups in hydrogen bonding suggests that the polarity (acidity) of the groups is greater than that of the phenyl C−H groups. However, perhaps most remarkable is the short (and presumably moderately strong) C−H···Cl hydrogen bond that links the chloroform solvate to the Cl ligand bound to Ag in **2a**. This reflects the enhanced polarity of the chloroform C−H bond relative to typical hydrocarbon C−H groups. At 2.47 Å, the H···Cl separation is some 0.48 Å less than the anticipated van der Waals contact for these atoms. A survey of the CSD[19] reveals some 40 observations of C−H···Cl hydrogen bonding involving chloroform solvate as the (hydrogen bond) donor group in which the H···Cl separation is less than 2.6 Å. In each case[20] the acceptor group chlorine is bound to a transition metal, which would be expected to give rise to greater charge accumulation on the Cl group than for organic chlorine. For comparison, the shortest H···Cl separation recorded is 2.29 Å in the chlorofrom solvate of a pentagonal-bipyramidal dichloro(10-crown-5)copper(II) compound.[21]

The Ag−Cl bond length in **2a**·$CHCl_3$, at 2.610(4) Å, is the longest reported in a *three-coordinate* organosilver compound, to our knowledge,[22] and warrants more detailed investigation. The CSD contains 24 structures with terminal Ag−Cl bonds, which range in length from 2.261 to 3.034 Å. Examination of these structures reveals two general trends: (i) increasing coordination number at Ag is associated with increasing Ag−Cl separation, and (ii) increasing Ag−Cl separation is associated with increased X−H···Cl−Ag hydrogen bonding (both in strength and in number of interactions).

(14) Braga, D.; Grepioni, F.; Sabatino, P.; Desiraju, G. R. *J. Am. Chem. Soc.* **1995**, *117*, 3156.
(15) Brammer, L.; Klooster, W. T.; Lemke, F. R. *Organometallics* **1996**, *15*, 1721.
(16) Brammer, L.; Charnock, J. M.; Goggin, P. L.; Goodfellow, R. J.; Orpen, A. G.; Koetzle, T. F. *J. Chem. Soc., Dalton Trans.*, **1991**, 1789.
(17) Braga, D.; Grepioni, F. *J. Chem. Soc., Chem. Commun.* **1996**, 571.
(18) (a) Desiraju, G. R. *Crystal Engineering: The Design of Organic Solids*; Elsevier: Amsterdam, 1989. (b) Desiraju, G. R. *Angew. Chem., Int. Ed. Engl.* **1995**, *34*, 2311.
(19) (a) See: Allen, F. H.; Kennard, O.; Taylor, R. *Acc. Chem. Res.* **1983**, *16*, 146. (b) The October 1995 version of CSD was used.
(20) Chloride ions were excluded as possible acceptor groups so as to focus only on bound chlorine substituents and ligands.
(21) Sakurai, T.; Kobayashi, K.; Tsuboyama, S.; Kohno, Y.; Azuma, N.; Ishizu, K. *Acta Crystallogr.* **1983**, *C39*, 206.
(22) (a) The mean terminal Ag−Cl bond length from the 18 structures [17, excluding the anomalously long Ag−Cl separations in structure AGSURE10[19a]] which meet the criteria for structure quality used by Orpen *et al.*[22b] is 2.506 [2.465], with the sample standard deviation $\sigma^{22b} = 0.182$ [0.121]. (b) Orpen, A. G.; Brammer, L.; Allen, F. H.; Kennard, O.; Watson, D. G.; Taylor, R. *J. Chem. Soc., Dalton Trans.* **1989**, S1−S83.

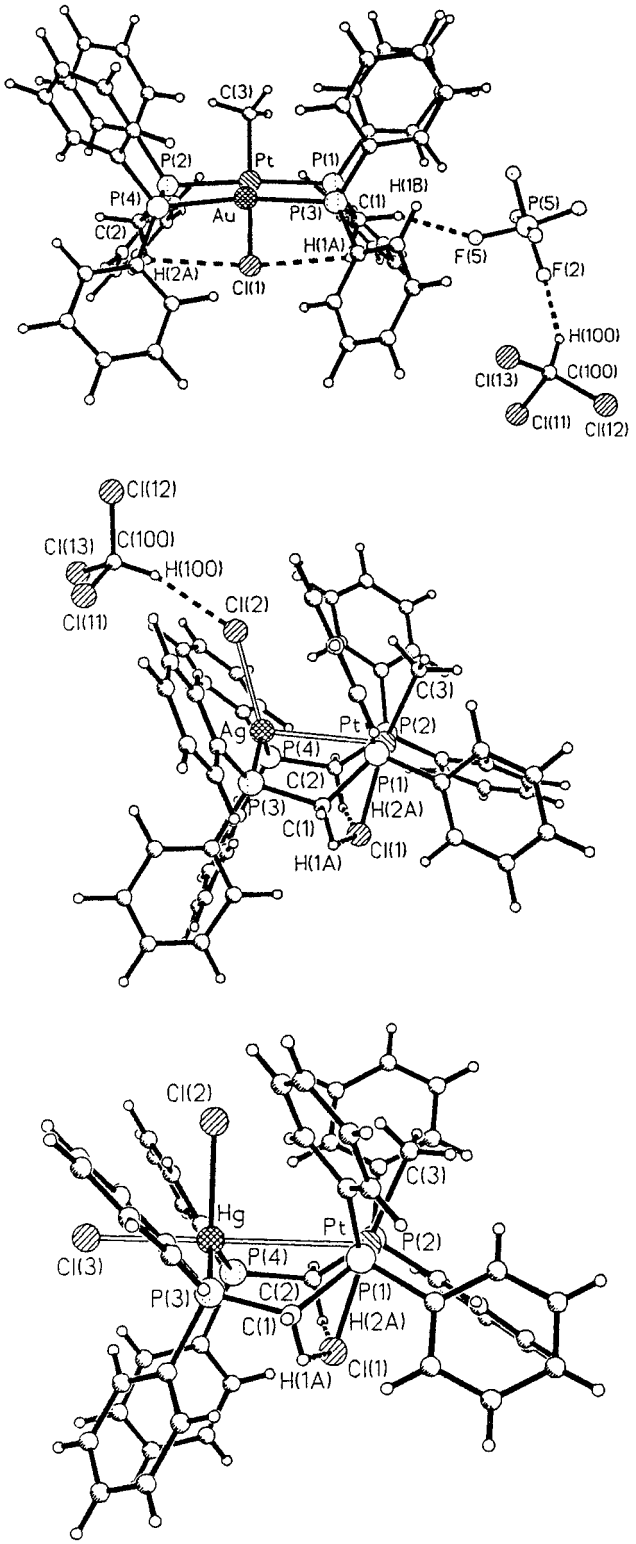

Figure 2. (Top to bottom) Molecular structures of **1**−**3**, depicting hydrogen-bonding interactions. Intermolecular interactions are indicated by bold dashed lines and intramolecular interactions by fine dashed lines. The C(2)−H(2b)···Cl(2) hydrogen bond linking molecules of **3** is not shown.

The latter can perhaps be rationalized in terms of greater $Ag^{\delta+}-Cl^{\delta-}$ charge separation upon lengthening the Ag−Cl bond. A summary is provided in the Supporting Information. There are some exceptions to these trends where other factors, such as coordination geometry in addition to coordination number, must also be taken into account. However, the trends suggest that the short $Cl_3C-H\cdots Cl-Ag$ hydrogen bond in **2a**·$CHCl_3$ may be an important factor in determining the Ag−Cl bond length.

Related to the above argument concerning the Ag−Cl bond length is the extent to which an attractive interaction between the metal centers is present. Nascent Pt−Ag bond formation could be regarded as an incipient S_N2 reaction at Ag in which the Pt center serves as the nucleophile and the chloride ligand, Cl(2), would serve as the leaving group. This is not to suggest that such a reaction could progress to completion, but merely that a weak attractive Pt···Ag interaction could contribute to elongation of the Ag−Cl bond. Consideration of the relative geometries of the two metal centers supports such an assertion. Both metals are displaced from the mean plane of their ligands[23] toward each other (Ag by 0.21 Å and Pt by 0.06 Å). The Pt−Ag vector makes an angle of 13.9° with the normal to the Pt ligand plane,[23] indicating that this direction is close to the orientation of the Pt $5d_{z^2}$ (and $6p_z$) orbitals. The Pt−Ag−P(3) and Pt−Ag−P(4) angles are 90.5(7) and 86.9(7)°, whereas the Pt−Ag−Cl(2) angle is 110.4(9)°. This can be interpreted to suggest that the chloride ligand is bent back away from the "approaching" Pt nucleophile, consistent with the suggested incipient S_N2 reaction at Ag. However, unlike the geometrically similar S_N2 reaction at a trigonal organic carbonyl carbon, in **2a** the sp^2-hybridized trigonal center (Ag) possess a donor ($5d_{z^2}$) in addition to its acceptor ($6p_z$) orbital. Thus incipient Pt−Ag bond formation could equally involve Ag→Pt electron donation. At 3.049(1) Å, the Pt···Ag separation is longer than a typical Pt−Ag single bond (mean 2.743 Å, range 2.637−2.893 Å),[19] and further analysis, including consideration of a repulsive interaction between the filled $5d_{z^2}$ orbitals of the two metal centers, would be necessary in order to provide definitive explanations for the questions posed by the observed geometry of **2a**.

The geometry about the Hg center in **3a** also warrants similar examination. The two phosphines and Cl(2) lie in an approximate trigonal plane with the axial chloride, Cl(3), oriented in a perpendicular direction, resulting in a trigonal-pyramidal arrangement. The Hg−Cl(2) bond length, at 2.531(5) Å, lies within the wide range of values typical of four-coordinate mercury species (2.28−2.68 Å,[19] mean[22b] 2.430 Å), while the axial Hg−Cl(3) bond, at 2.715(4) Å, is the longest *terminal* Hg−Cl bond yet observed in an organomercury compound.[19] Indeed, we were able to find only one compound with a longer terminal Hg−Cl bond (2.968 Å), involving the five-coordinate mercury center in the anion of $[Co(en)_2(NH_3)(py)][Hg_2Cl_7]$.[24,25] The elongated Hg−Cl(3) bond in **3a** may perhaps best be explained in terms of the hybridization at Hg, in which one can view the three equatorial ligands as interacting with a set of $6sp^2$ hybrid orbitals on Hg and the axial chloride interacts with the more radially diffuse $6p_z$ orbital. Auxiliary contributions to the lengthening of the axial Hg−Cl(3) bond might be considered to arise from intermolecular short C−H···Cl hydrogen bonding

(23) Mean planes of P(3)−P(4)−Cl(2) for Ag and P(1)−P(2)−Cl(1)−C(3) for Pt.

(24) House, D. A.; McKee, V.; Robinson, W. T. *Inorg. Chim. Acta* **1989**, *160*, 71.

Table 2. Interatomic Distances[a] (Å) and Angles[a] (deg) for Hydrogen Bonds[b] in 1−3

Intramolecular H Bonds

	1	2	3
Cl(1)···H(1a)	2.81	2.65	2.69
Cl(1)···H(2a)	2.90	2.78	2.82
Pt−Cl(1)···H(1a)	89	88	89
C(1)−H(1a)···Cl(1)	109	116	109
Pt−Cl(1)···H(2a)	88	88	90
C(2)−H(2a)···Cl(1)	106	107.5	102.5
H(1a)···Cl(1)···H(2a)	151	156	162

Intermolecular H Bonds

1		2		3	
H(52)···F(2)	2.34	H(52)···Cl(2)	2.47	H(2b)···Cl(2)	2.73
C(52)−H(52)···F(2)	156	C(52)−H(52)···Cl(2)	163	C(2)−H(2b)···Cl(2)	135
P(3)−F(2)···H(52)	123	Ag−Cl(2)···H(52)	139	Hg−Cl(2)···H(2b)	159
H(1a)···F(5)	2.29				
C(1)−H(1a)···F(5)	151				
P(3)−F(5)···H(1a)	155				

[a] Calculated on the basis of C−H bonds extended to 1.09 Å. [b] Sum of van der Waals radii for H + F is 2.67 Å, and for H + Cl is 2.95 Å.

(albeit weak), and as in **2a** from invoking nascent Pt−Hg bond formation[26] and therefore an incipient S_N2 reaction[27] at Hg in which Cl(3) would serve as the leaving group.

Variable-Temperature NMR Studies. Each of the complexes under study exhibited two well-separated, but poorly resolved, multiplets due to the CH_2 hydrogens of the bridging dppm ligands in its ^1H NMR spectrum at ambient temperature. This is to be expected, irrespective of the conformation of the eight-membered $Pt(P-C-P)_2M$ ring in solution, because one hydrogen will lie on the same side of the ring as the Pt−Cl bond and the other hydrogen will lie on the opposite side. Qualitatively similar observations have been made for a number of dppm-bridged species.[10,11,28−31]

When 1,1,2,2-tetrachloroethane-d_2 solutions of the methyl- and phenylplatinum complexes were heated above ambient temperature, the dppm CH_2 resonances broadened further and eventually coalesced into one broad, featureless signal. In each case the coalescence temperature was obtained and $\Delta G^{\ddagger}$ for the exchange process was calculated.[32] (The ethyl complexes decomposed extensively on heating, and coalescence temperatures could not be determined.) The Pt−Ag and Pt−Hg complexes exhibited similar behavior (**2a**, $T_c = 343$ K, $\Delta G^{\ddagger} = 15.3 \pm 0.1$ kcal/mol; **2c**, $T_c = 303$ K, $\Delta G^{\ddagger} = 13.4 \pm 0.1$ kcal/mol; **3a**, $T_c = 341$K, $\Delta G^{\ddagger} = 15.3 \pm 0.1$ kcal/mol; **3c**, $T_c = 305$ K, 13.7 ± 0.1 kcal/mol), the free energy of activation being nearly 2 kcal/mol higher in the methylplatinum complexes. Whereas the ^1H NMR spectra of the Pt−Au complexes also revealed a higher $\Delta G^{\ddagger}$ value for the methyl complex, albeit by only 1 kcal/mol in this case (**1a**, $T_c = 415$ K, $\Delta G^{\ddagger} = 19.3 \pm 0.2$ kcal/mol; **1c**, $T_c = 389$ K, $\Delta G^{\ddagger} = 18.2 \pm 0.1$ kcal/mol), the $\Delta G^{\ddagger}$ values were 4−5 kcal/mol higher than in the Pt−Ag and Pt-Hg species.

We interpret this NMR behavior to indicate that the complexes are static at ambient temperature, at least in terms of inversion about the $Pt(P-C-P)_2M$ ring, but at higher temperatures the molecules are fluxional. This fluxional behavior renders the two dppm CH_2 hydrogens equivalent on the NMR time scale. It has been shown that dppm-bridged A-frame complexes of platinum of the type $[Pt_2R_2(\mu\text{-}X)(\mu\text{-dppm})_2]^+$ undergo inversion of the A-frame structure at ambient temperature, presumably *via* a linear R−Pt−X−Pt−R intermediate, when X = H, but not when X = Cl.[33] The bridging hydrogen can pass through the center of the $Pt(P-C-P)_2Pt$ ring, but the bridging chloride is too large to do so. In fact, we have heated solutions of the $[Pt_2Me_2(\mu\text{-Cl})(\mu\text{-dppm})_2]^+$ cation to 343 K and the two CH_2 signals remained sharp, indicating that no fluxional motion occurs even at this temperature. In the present complexes **1**−**3**, rotation about the P−Pt−P axis would render the CH_2 hydrogens equivalent. Such a mechanism is ruled out, however, because it would require the Cl or CH_3 (or Ph) to pass through the eight-membered $Pt(P-C-P)_2M$ ring. Alternative mechanisms could involve (1) Pt−P bond cleavage, followed by rotation of the resulting three-coordinate PtPClR unit and reattachment of the phosphino group, or (2) dissociation of chloride, followed by rotation about the P−Pt−P axis and coordination of Cl^- to the opposite face of the molecule. We cannot distinguish unambiguously between these mechanisms, but the higher $\Delta G^{\ddagger}$ values observed for the cationic Pt−Au complexes support the latter, since we would expect that Cl^- dissociation from an already positively charged species would represent a higher energy process. The proposed mechanism is illustrated in eq 4. A mecha-

(25) Consistent with arguments on hydrogen bonding presented earlier, the chloride ligand in this salt participates in a number of short N−H···Cl interactions and might even be thought of as a Cl^- anion that is weakly coordinated to the Hg center.

(26) Typical Pt−Hg single-bond lengths lie in the range[19] 2.510−2.835 Å (mean 2.658 Å).

(27) (a) Such a reaction has been described by Bürgi[27b] for Cd(II) centers in an application of the Structure Correlation Method.[27c] (b) Bürgi, H.-B. *Inorg. Chem.* **1973**, *12*, 2321. (c) Bürgi, H.-B.; Dunitz, J. D. *Acc. Chem. Res.* **1983**, *16*, 153.

(28) Brown, M. P.; Fisher, J. R.; Puddephatt, R. J.; Seddon, K. R. *Inorg. Chem.* **1979**, *18*, 2808.

(29) Langrick, C. R.; Pringle, P. R.; Shaw, B. L. *J. Chem. Soc., Dalton Trans.* **1985**, 1015.

(30) Hutton, A. T.; Langrick, C. R.; McEwan, D. M.; Pringle, P. R.; Shaw, B. L. *J. Chem. Soc., Dalton Trans.* **1985**, 2121.

(31) Neve, F.; Ghedini, M.; De Munno, G.; Crispini, A. *Inorg. Chem.* **1992**, *31*, 2979.

(32) Martin, M. L.; Delpuech, J.-J.; Martin, G. J. *Practical NMR Spectroscopy*; Heydon: London, 1980; p 340.

(33) Puddephatt, R. J.; Azam, K. A.; Hill, R. H.; Brown, M. P.; Nelson, C. D.; Moulding, R. P.; Seddon, K. R.; Grossel, M. C. *J. Am. Chem. Soc.* **1983**, *105*, 5642.

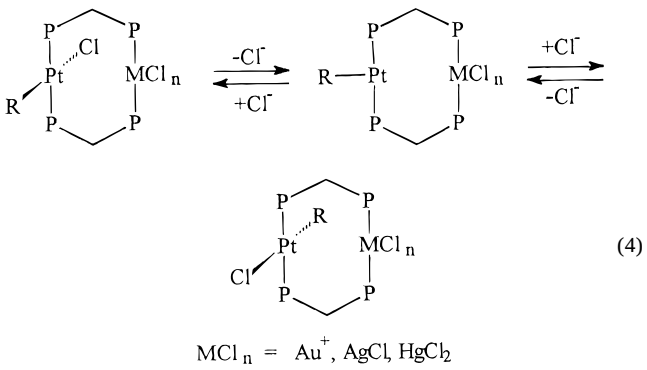

MCl_n = Au^+, AgCl, $HgCl_2$ (4)

nism involving halide dissociation has been proposed previously to account for the fluxional behavior observed in the face-to-face palladium dimers $[Pd_2X_2R_2(\mu\text{-dppm})_2]$ (X = Br, R = Me; X = I, R = Me, COMe).[34]

Summary

The $[PtR(dppm\text{-}P,P)(dppm\text{-}P)]^+$ cations (R = Me, Et, Ph) have been employed in the synthesis of the series of dppm-bridged heterobimetallic complexes *trans*-$[PtClR(\mu\text{-dppm})_2MCl_n]$ (MCl_n = Au^+, AgCl, $HgCl_2$), which were isolated in good yield. The Pt−Au species were prepared by reaction of $[AuCl(SMe_2)]$ with the cations as their hexafluorophosphate salts, whereas the Pt−Ag and Pt−Hg derivatives required initial reaction of $[PtR(dppm\text{-}P,P)(dppm\text{-}P)]Cl$ with AgOAc or $Hg(OAc)_2$, followed by addition of acetyl chloride. Each of the methylplatinum complexes has been characterized by X-ray crystallography, and the molecular structures reveal linear, trigonal, and tetrahedral geometries at the gold, silver, and mercury centers, respectively. The last two exhibit unusually long Ag−Cl (2.610(4) Å) and Hg−Cl (2.716(4) Å) bonds. These appear to be associated with a moderately strong $Cl_3C-H\cdots Cl-Ag$ hydrogen bond in one case and hybridization of the mercury valence orbitals in the other. However, both might be viewed in terms of an incipient metal-centered S_N2 reaction resulting in nascent Pt···M bond formation and M−Cl bond weakening. The complexes are static in solution at ambient temperature, but they exhibit fluxional behavior at higher temperatures which renders the dppm CH_2 hydrogens equivalent on the NMR time scale. A mechanism involving reversible chloride dissociation is proposed to account for this behavior.

Experimental Section

All reactions were carried out under an atmosphere of argon. Complexes of the type $[PtR(dppm\text{-}P,P)(dppm\text{-}P)]PF_6$ (R = Me, Et, Ph) were prepared as described previously. Routine ^1H and $^{31}P\{^1H\}$ NMR spectra were recorded on a Varian XL-300 spectrometer. Variable-temperature NMR spectra were recorded on a Bruker ARX-500 spectrometer. Microanalyses were performed by Atlantic Microlab, Inc., Norcross, GA.

Preparation of *trans*-$[PtClMe(\mu\text{-dppm})_2Au]PF_6$ (1a). $[AuCl(SMe_2)]$ (0.030 g, 0.10 mmol) was dissolved in CH_2Cl_2 (5 mL), and a CH_2Cl_2 solution (5 mL) of $[PtMe(dppm\text{-}P,P)(dppm\text{-}P)]PF_6$ (0.112 g, 0.10 mmol) was added dropwise. NH_4PF_6 (0.033 g, 0.20 mmol) was added as a solid, followed by methanol (2.5 mL), and the mixture was stirred at ambient temperature for 1 h. The solvents were removed, and the residue was washed several times with pentane and then extracted into CH_2Cl_2 (10 mL). The resulting solution was passed through a column of Hyflo Supercel, and the column was washed with further CH_2Cl_2 (15 mL). The resulting solution was evaporated to dryness, washed with small portions of pentane and ether, and dried in vacuo, leaving the product as a pale yellow powder (0.120 g, 88%). Anal. Found: C, 44.72; H, 3.57. Calcd for $C_{51}H_{47}AuClF_6P_5Pt$: C, 45.16; H, 3.49. ^1H NMR ($CDCl_3$): δ(H) 0.47 t, $^3J(P,H) = 6$ Hz, $^2J(Pt,H) = 78$ Hz (CH_3); 4.0 br, 4.4 br (PCH_2P); 7.0−7.9 m (C_6H_5). $^{31}P\{^1H\}$ NMR: δ(P) 19.8 t, $^1J(Pt,P) = 3049$ Hz, $|^2J(P,P) + {}^4J(P,P)| = 49$ Hz; δ(P) 29.8 t, $^3J(Pt,P) = 126$ Hz. Crystals suitable for X-ray diffraction were grown from $CHCl_3$ solution.

trans-$[PtClEt(\mu\text{-dppm})_2Au]PF_6$ (**1b**) was prepared similarly and isolated as a pale yellow powder in 87% yield. Anal. Found: C, 45.54; H, 3.62. Calcd for $C_{52}H_{49}AuClF_6P_5Pt$: C, 45.58; H, 3.60. ^1H NMR ($CDCl_3$): δ(H) 0.38 t, $^3J(H,H) = 7$ Hz (CH_3); 1.08 q (CH_2); 4.1 br, $^3J(Pt,H) = 38$ Hz, 4.4 br (PCH_2P); 7.1−8.0 m (C_6H_5). $^{31}P\{^1H\}$ NMR: δ(P) 21.1 t, $^1J(Pt,P) = 3292$ Hz, $|^2J(P,P) + {}^4J(P,P)| = 48$ Hz; δ(P) 29.9 t, $^3J(Pt,P) = 142$ Hz.

trans-$[PtClPh(\mu\text{-dppm})_2Au]PF_6$ (**1c**) was prepared similarly and isolated as a pale yellow powder in 87% yield. Anal. Found: C, 47.51; H, 3.45. Calcd for $C_{56}H_{49}AuClF_6P_5Pt$: C, 47.42; H, 3.48. ^1H NMR ($CDCl_3$): δ(H) 3.7 br, 4.3 br (PCH_2P); 6.7−8.0 m (C_6H_5). $^{31}P\{^1H\}$ NMR ($CDCl_3$, −50 °C): δ(P) 16.3 t, $^1J(Pt,P) = 3026$ Hz, $|^2J(P,P) + {}^4J(P,P)| = 55$ Hz; δ(P) 30.5 t, $^3J(Pt,P) = 139$ Hz.

Preparation of *trans*-$[PtClMe(\mu\text{-dppm})_2AgCl]$ (2a). Silver(I) acetate (0.017 g, 0.10 mmol) was suspended in CH_2Cl_2 (5 mL), and a CH_2Cl_2 solution (5 mL) of $[PtMe(dppm\text{-}P,P)(dppm\text{-}P)]Cl$ (0.101 g, 0.10 mmol) was added dropwise. The solid gradually dissolved to give a clear, colorless solution. After 1 h, a CH_2Cl_2 solution (5 mL) of acetyl chloride (2 drops) was added dropwise, and the reaction was allowed to continue for a further 15 min. The solvent was evaporated, and the solid residue was washed with pentane. The solid was redissolved in CH_2Cl_2 (10 mL), and the resulting solution was passed through a column of Hyflo Supercel. The column was rinsed with further CH_2Cl_2 (15 mL). The solutions were combined and evaporated to dryness. The resulting solid was washed with pentane and dried in vacuo, leaving the product as a white powder (0.110 g, 96%). Anal. Found: C, 53.02; H, 4.14. Calcd for $C_{51}H_{47}AgCl_2P_4Pt$: C, 52.91; H, 4.09. ^1H NMR ($CDCl_3$): δ(H) 0.84 t, $^3J(P,H) = 6$ Hz, $^2J(Pt,H) = 84$ Hz (CH_3); 3.4 br, 4.5 br (PCH_2P); 7.0−8.0 m (C_6H_5). $^{31}P\{^1H\}$ NMR: δ(P) 24.0 dd, $^1J(Pt,P) = 3034$ Hz, $|^2J(P,P) + {}^4J(P,P)| = 96$ Hz; δ(P) 10.0 dddd, $^1J(^{109}Ag,P) = 458$ Hz, $^1J(^{107}Ag,P) = 397$ Hz. Crystals suitable for X-ray diffraction were grown from $CHCl_3$ solution.

trans-$[PtClEt(\mu\text{-dppm})_2AgCl]$ (**2b**) was prepared similarly and isolated as a white powder in 90% yield. Anal. Found: C, 53.41; H, 4.28. Calcd for $C_{52}H_{49}AgCl_2P_4Pt$: C, 53.30; H, 4.22. ^1H NMR ($CDCl_3$): δ(H) 0.64 t, $^3J(H,H) = 8$ Hz, $^3J(Pt,H) = 63$ Hz (CH_3); 1.67 q, $^2J(Pt,H) = 78$ Hz (CH_2); 3.4 br, 4.5 br (PCH_2P); 7.0−8.0 m (C_6H_5). $^{31}P\{^1H\}$ NMR: δ(P) 24.7 dd, $^1J(Pt,P) = 3261$ Hz, $|^2J(P,P) + {}^4J(P,P)| = 94$ Hz; δ(P) 10.1 dddd, $^1J(^{109}Ag,P) = 456$ Hz, $^1J(^{107}Ag,P) = 396$ Hz.

trans-$[PtClPh(\mu\text{-dppm})_2AgCl]$ (**2c**) was prepared similarly and isolated as a white powder in 83% yield. Anal. Found: C, 54.84; H, 4.10. Calcd for $C_{56}H_{49}AgCl_2P_4Pt$: C, 55.14; H, 4.05. ^1H NMR ($CDCl_3$, −40 °C): δ(H) 3.3 br, 4.4 br (PCH_2P); 6.7−8.0 m (C_6H_5). $^{31}P\{^1H\}$ NMR ($CDCl_3$, −50 °C): δ(P) 21.6 dd, $^1J(Pt,P) = 3033$ Hz, $|^2J(P,P) + {}^4J(P,P)| = 94$ Hz; δ(P) 8.9 dddd, $^1J(^{109}Ag,P) = 461$ Hz, $^1J(^{107}Ag,P) = 399$ Hz.

Preparation of *trans*-$[PtClMe(\mu\text{-dppm})_2HgCl_2]$ (3a). A CH_2Cl_2 solution (5 mL) of $[PtMe(dppm\text{-}P,P)(dppm\text{-}P)]Cl$ (0.101 g, 0.10 mmol) was added dropwise to a suspension of mercury(II) acetate in CH_2Cl_2 (5 mL). The solid dissolved gradually to give a clear yellow solution. After 1 h, a solution of acetyl chloride (2 drops) in CH_2Cl_2 (5 mL) was introduced dropwise, and the solution changed from yellow to colorless. After a

(34) Balch, A. L.; Hunt, C. T.; Lee, C.-L.; Olmstead, M. M.; Farr, J. P. *J. Am. Chem. Soc.* **1981**, *103*, 3764. Lee, C.-L.; Hunt, C. T.; Balch, A. L. *Organometallics* **1982**, *1*, 824.

Table 3. Data Collection, Structure Solution, and Refinement Parameters for 1−3

	1	2	3
cryst system	orthorhombic	monoclinic	orthorhombic
space group, Z	$P2_12_12_1$, 4	$C2/c$, 8	$P2_12_12_1$, 4
a (Å)	10.685(2)	39.749(11)	10.011(1)
b (Å)	18.817(6)	13.027(4)	16.572(1)
c (Å)	27.366(4)	21.928(7)	28.243(1)
β (deg)		115.50(2)	
V (Å^3)	5502(2)	10 248(5)	4685.3(1)
density (g/cm^3)	1.781	1.655	1.823
temp (K)	295(2)	295(2)	143(5)
μ(Mo Kα)[a] (mm^{-1})	5.598	3.530	6.598
diffractometer	Siemens R3m/V	Siemens R3m/V	Siemens SMART CCD
θ range (deg)	1.84−25.06	1.66−27.56	1.42−26.50
no. of rflns collected	5841	12 540	43 815
no. of indep rflns (R_{int})	5668 (0.020)	11 845 (0.050)	9715 (0.078)
ls params	604	568	320
abs structure param,[b] x	−0.01(1)	n.a.	0.01(1)
$R(F)$, $R_w(F^2)$ ($F^2 > 2.0\sigma(F^2)$)[c]	0.055, 0.093	0.075, 0.113	0.077, 0.206
$R(F)$, $R_w(F^2)$ (all data)[c]	0.098, 0.108	0.171, 0.145	0.085, 0.214
$S(F^2)$ (all data)[c]	1.03	1.00	1.84

[a] Graphite-monochromated X-rays, wavelength 0.710 73 Å. [b] Flack parameter (Flack, H. *Acta Crystallogr.* **1983**, *A39*, 876). [c] $R(F) = \Sigma||F_o| - |F_c||/\Sigma|F_o|$; $R_w(F^2) = [\Sigma w(F_o^2 - F_c^2)^2/\Sigma wF_o^4]^{1/2}$; $S(F^2) = [\Sigma w(F_o^2 - F_c^2)^2/(n - p)]^{1/2}$.

further 15 min the solvent was removed, and the solid residue was washed with several small portions of pentane. The solid was redissolved in CH_2Cl_2 (10 mL), and the resulting solution was passed through a Hyflo Supercel column. The column was washed with further CH_2Cl_2 (15 mL), and the combined solution was evaporated to dryness. The resulting solid was washed with pentane and then dried in vacuo, leaving the product as a white powder (0.105 g, 82%). Anal. Found: C, 47.37; H, 3.70. Calcd for $C_{51}H_{47}Cl_3HgP_4Pt$: C, 47.64; H, 3.68. ^{1}H NMR ($CDCl_3$): δ(H) 0.77 t, ^3J(P,H) = 5 Hz, ^2J(Pt,H) = 82 Hz (CH_3); 3.75 br, 4.7 br (PCH_2P); 7.0−8.2 m (C_6H_5). ^{31}P{^{1}H} NMR: δ(P) 22.3 t, ^1J(Pt,P) = 3135 Hz, ^3J(Hg,P) = 45 Hz, $|^2J(P,P) + {}^4J(P,P)|$ = 64 Hz; δ(P) 15.6 t, ^1J(Hg,P) = 5657 Hz, ^3J(Pt,P) = 227 Hz. Crystals suitable for X-ray diffraction were grown from $CHCl_3$ solution.

trans-[PtClEt(μ-dppm)$_2$HgCl$_2$] (**3b**) was prepared similarly and isolated as a white powder in 73% yield. Found: C, 47.98; H, 3.91. Anal. Calcd for $C_{52}H_{49}Cl_3HgP_4Pt$: C, 48.05; H, 3.80. ^{1}H NMR ($CDCl_3$): δ(H) 0.60 t, ^3J(H,H) = 8 Hz, ^3J(Pt,H) = 66 Hz (CH_3); 1.63 q (CH_2); 3.7 br, 4.7 br (PCH_2P); 7.1−8.2 m (C_6H_5). ^{31}P{^{1}H} NMR: δ(P) 23.1 dd, ^1J(Pt,P) 3371 Hz, ^3J(Hg,P) = 46 Hz, $|^2J(P,P) + {}^4J(P,P)|$ = 63 Hz; δ(P) 15.2 dd, ^1J(Hg,P) = 5614 Hz, ^3J(Pt,P) = 253 Hz.

trans-[PtClPh(μ-dppm)$_2$HgCl$_2$] (**3c**) was prepared similarly and isolated as a white powder in 84% yield. Anal. Found: C, 49.63; H, 3.77. Calcd for $C_{56}H_{49}Cl_3HgP_4Pt$: C, 49.90; H, 3.66. ^{1}H NMR ($CDCl_3$, −40 °C): δ(H) 3.6 br, 4.5 br (PCH_2P); 6.8−8.1 m (C_6H_5). ^{31}P{^{1}H} NMR ($CDCl_3$): δ(P) 18.1 br t, ^1J(Pt,P) = 3140 Hz, ^3J(Hg,P) = 56 Hz, $|^2J(P,P) + {}^4J(P,P)|$ = 54 Hz; δ(P) 15.8 br t, ^1J(Hg,P) = 5701 Hz, ^3J(Pt,P) = 185 Hz.

X-ray Crystal Structure Determinations of [PtClMe(μ-dppm)$_2$Au]PF$_6$·CHCl$_3$ (1a·CHCl$_3$), [PtClMe(μ-dppm)$_2$AgCl]·CHCl$_3$ (2a·CHCl$_3$), and [PtClMe(μ-dppm)$_2$HgCl$_2$] (3a). The crystal structures were solved by Patterson methods and subsequently refined to convergence by full-matrix least squares using the SHELXTL suites of programs.[35] In each case a semiempirical correction for the effects of absorption was applied on the basis of ψ-scan (**1a**·$CHCl_3$ and **2a**·$CHCl_3$) or symmetry-equivalent (**3a**) data. In the latter case the calculated correction was minor, despite the clear suggestion of absorption effects manifested in large residual density peaks ca. 1 Å from the metal atoms. The presence of low-angle reflections with $F_o^2 > F_c^2$ suggested an additional contribution to these reflections from a twin component. However, despite measurement of a number of data sets from different crystals and at different temperatures, we were unable to model this contribution, which necessarily rendered the absorption correction less effective. For **1a**·$CHCl_3$ and **2a**·$CHCl_3$, all non-hydrogen atoms were refined anisotropically; hydrogens were included in calculated positions and treated using a riding model constraint with fixed isotropic displacement parameters. For **3a**, an unconstrained model for the non-hydrogen atoms led to chemically unreasonable geometries within the phenyl groups. Thus, the final model included constraints on these groups: the ring geometry was constrained to be a regular hexagon, and *ortho* and *meta* carbons were constrained to have anisotropic displacement parameters identical with those of the carbon opposite in the ring. No systematic changes in geometry or displacement parameters of the PtClMe(P−C−P)$_2$-$HgCl_2$ core were observed in changing from the (unreasonable) unconstrained model to the final (constrained) model. Hydrogen atoms were treated in the same manner as for **1a**·$CHCl_3$ and **2a**·$CHCl_3$. Experimental data pertinent to these structure determinations are given in Table 3.

Variable-Temperature NMR Experiments. ^{1}H NMR spectra were recorded in 1,1,2,2-tetrachloroethane-d_2 solution, and the CH_2 resonance of the dppm ligand was monitored. In the slow exchange regime two signals were observed, and the frequency difference ($\Delta\nu$) for the two hydrogens at the coalescence temperature (T_c) was obtained by extrapolation from the low-temperature data. Exchange rate constants, k_c, at the coalescence temperature were calculated using the equation $k_c = \pi(\Delta\nu)/2^{1/2}$. The exchange constants were used to determine $\Delta G^{\ddagger}$ at the coalescence temperature from the Eyring equation $k_c = (k'/h)T_c \exp(-\Delta G^{\ddagger}/RT_c)$, where k' = Boltzmann's constant, h = Planck's constant, and R = the ideal gas constant.[32]

Acknowledgment. Thanks are expressed to the National Science Foundation (Grant Nos. CHE-9101834 and CHE-9508228), the donors of the Petroleum Research Fund, administered by the American Chemical Society, and the University of Missouri−St. Louis for support of this work and to Johnson Matthey Aesar/Alfa for generous loans of platinum salts. C.X. acknowledges the receipt of a Dissertation Fellowship from the University of Missouri−St. Louis.

Supporting Information Available: Tables of X-ray crystallographic data, positional parameters, anisotropic displacement parameters, and interatomic distances and angles for **1a**·$CHCl_3$, **3a**·$CHCl_3$, and **3a** (24 pages). Ordering information is given on any current masthead page.

OM960355K

(35) SHELXTL 5.0; Siemens Analytical X-ray Instruments Inc., Madison, WI, 1995.